

RESEARCH ARTICLE

Metformin partially reverses the inhibitory effect of co-culture with ER⁻/PR⁻/HER2⁺ breast cancer cells on biomarkers of monocyte antitumor activity

Zoheir Dahmani¹, Lynda Addou-Klouche¹, Florence Gizard^{1,2}, Sara Dahou¹, Aida Messaoud¹, Nihel Chahinez Djebri¹, Mahmoud Idris Benaissi¹, Meriem Mostefaoui¹, Hadjer Terbeche¹, Wafa Nouari¹, Marwa Miliani¹, Gérard Lefranc³, Anne Fernandez², Ned J. Lamb^{2*}, Mourad Aribi^{1*}

1 Laboratory of Applied Molecular Biology and Immunology, W0414100, University of Tlemcen, Tlemcen, Algeria, **2** Cell Biology Unit, IGH CNRS, Université de Montpellier, (UMR 9002), Montpellier, France, **3** IGH, UMR 9002 CNRS-Université de Montpellier, Montpellier, France

* mourad.aribi@univ-tlemcen.dz, m_aribi@outlook.fr, m_aribi@yahoo.fr (MA); ned.lamb@igh.cnrs.fr (NJL)



OPEN ACCESS

Citation: Dahmani Z, Addou-Klouche L, Gizard F, Dahou S, Messaoud A, Chahinez Djebri N, et al. (2020) Metformin partially reverses the inhibitory effect of co-culture with ER⁻/PR⁻/HER2⁺ breast cancer cells on biomarkers of monocyte antitumor activity. *PLoS ONE* 15(10): e0240982. <https://doi.org/10.1371/journal.pone.0240982>

Editor: Salvatore V Pizzo, Duke University School of Medicine, UNITED STATES

Received: April 28, 2020

Accepted: October 6, 2020

Published: October 27, 2020

Copyright: © 2020 Dahmani et al. This is an open access article distributed under the terms of the [Creative Commons Attribution License](https://creativecommons.org/licenses/by/4.0/), which permits unrestricted use, distribution, and reproduction in any medium, provided the original author and source are credited.

Data Availability Statement: All relevant data are within the manuscript and its Supporting Information files.

Funding: This work was funded by the Thematic Research Agencies ATRBSA and ATRSS (Algeria) and the Directorate General of Scientific Research and Technological Development (DGRSDT, Direction Générale de la Recherche Scientifique et du Développement Technologique, MESRS, Algeria) for financial support to ZD, LA-K, SD, AM,

Abstract

Background

Immune activities of monocytes (MOs) can be altered within the microenvironment of solid malignancies, including breast cancer. Metformin (1,1-dimethylbiguanide hydrochloride, MET), has been shown to decrease tumor cell proliferation, but its effects have yet to be explored with respect to MOs (monocytes) activity during their crosstalk with breast cancer cells. Here, we investigated the effects of MET on overall phenotypic functional activities, including cellular immunometabolism and protective redox signaling based-biomarkers, intracellular free calcium ions ($_{i}Ca^{2+}$), phagocytosis and co-operative cytokines (IFN- γ and IL-10) of autologous MOs before and during their interplay with primary ER⁻/PR⁻/HER2⁺ breast cancer cells.

Methods

Human primary breast cancer cells were either cultured alone or co-cultured with autologous MOs before treatment with MET.

Results

MET downregulated breast cancer cell proliferation and phagocytosis, while having no significant effect on the ratio of phosphorylated Akt (p-Akt) to total Akt. Additionally, we observed that, in the absence of MET treatment, the levels of lactate dehydrogenase (LDH)-based cytotoxicity, catalase, $_{i}Ca^{2+}$, IL-10 and arginase activity were significantly reduced in co-cultures compared to levels in MOs cultured alone whereas levels of inducible nitric oxide synthase (iNOS) activity were significantly increased. In contrast, MET treatment reduced the effects measured in co-culture on the levels of LDH-based cytotoxicity, arginase activity, catalase, $_{i}Ca^{2+}$, and IFN- γ . MET also induced upregulation of both iNOS and

NC-D, MI-B, MM, HT, WN, MM and MA. FG, GL, AF and NL were supported by CNRS core funding and AFD (Association Francaise pour la Diabete) grant 1546. The funders had no role in study design, data collection and analysis, decision to publish, or preparation of the manuscript.

Competing interests: The authors have declared that no competing interests exist.

arginase in MO cells, although the increase did not reach significant difference for iNOS activity. Moreover, MET induced a robust increase of superoxide dismutase (SOD) activity in MOs, but not in MOs co-cultured with breast cancer cells. Furthermore, MET markedly upregulated the levels of IFN- γ production and downregulated those of IL-10 in isolated MOs, while inducing a slight opposing up-regulation of IL-10 production in co-cultures.

Conclusions

Our results show that the biomarkers of phenotypic functional activities of MOs are modified after co-culturing with primary human breast cancer cells. Treatment of co-cultures with MET resulted in increased release of antitumor cytokine IFN- γ and Ca^{2+} , and increased cell necrosis during breast cancer cells-MOs crosstalk.

Introduction

Breast cancer is the most commonly diagnosed cancer and a leading cause of mortality worldwide [1]. Compared to other types of cancer that are considered as more responsive to immunotherapy, breast cancer has not been traditionally considered as an immunogenic malignancy [2]. However, recent research has shown the relationship between immune intra-tumoral responses and breast cancer development [3]. Additionally, studies reported that infiltration of immune cells within the tumor microenvironment and the presence of immunity-related gene signatures contribute to breast cancer prognosis [4,5].

The microenvironment surrounding breast cancer cells plays an important role in modulating cancer growth and progression [3]. It contains several types of inflammatory cells including MOs and macrophages. MO cells represent a heterogeneous population derived from myeloid lineages [6] that are recruited from the bloodstream to the tumor site through the paracrine action of cytokines and chemokines released by breast cancer cells [7]. Previous reports suggested that infiltration of MOs into the breast tumor microenvironments, in response to paracrine stimulation, correlates with poor prognosis and promotion of tumor growth, invasion and metastasis [8,9].

In light of their functional phenotypic plasticity, MOs can be targeted by several therapeutic molecules that switch them towards proinflammatory/anti-tumoral killer cells [10,11], which are mainly implicated in inflammatory response, thereby having reduced phagocytic capacity [12]. In context of cancer, these cells exert their inhibitory effects by enhanced production of proinflammatory cytokines, like IFN- γ , secretion of tumoricidal mediators, reactive oxygen (ROS) and nitrogen species (RNS), including the production of nitric oxide (NO) as product of the NOS activation [13].

It is well known that insulin is an important growth factor, which plays a critical role in regulation of cell proliferation. As such, enhancing insulin sensitivity can lead to tumor growth inhibition and cell cycle arrest. Indeed, metformin (1,1-dimethylbiguanide hydrochloride, MET), an antidiabetic drug prescribed for patients with type 2 diabetes [14,15], has been reported to have a marked effect on insulin sensitivity through inhibition of the signaling pathway implicating phosphoinositol-3-kinase (PI3K) and Akt (also referred to as protein kinase B, PKB) consequently leading to decreased tumor cell proliferation [16,17]. The effects of MET on breast cancer cells has also been associated with the inhibition of pro-tumoral M2-like macrophage polarization [18]. In this context, we investigated for the first time the

effects of MET on the overall phenotypic functional activities, including immunometabolic (arginase activity, iNOS activity and LDH release) [19] and protective redox based-biomarkers (catalase and SOD activities) [20], $_{i}Ca^{2+}$, phagocytosis, and co-operative cytokines (IFN- γ and IL-10) [21] of autologous MOs before and during their crosstalk with breast cancer cells (ER⁻/PR⁻/HER2⁺).

Materials and methods

Materials

Unless specified, all materials including (MET), were obtained from Sigma-Aldrich (Sigma Chemical Co., St. Louis, USA).

1. Study design. Tumor epithelial cells were isolated from breast cancer tissue specimens, and co-cultured with autologous MOs, isolated from peripheral blood mononuclear cells (PBMCs). First, tumor cells were cultured alone to check the MET effects on both proliferation and viability using BrdU (Bromodeoxyuridine [5-bromo-2'-deoxyuridine]), and Trypan Blue Exclusion Test [TBET], respectively, and on p-Akt-to-Akt ratios. Similarly, MOs were cultured alone for phagocytosis capacity assays. LDH-based cytotoxicity, respiratory burst and redox activity (nitric oxide [NO], catalase, superoxide dismutase [SOD]), release of co-operative cytokines ('antitumor cytokine IFN- γ ', and 'immunosuppressive/regulatory cytokine IL-10'), inducible nitric oxide synthase iNOS-associated proinflammatory MOs and arginase activities-associated anti-inflammatory MOs, and intracellular free calcium ions ($_{i}Ca^{2+}$) were measured in MOs cultured alone and co-cultured with breast cancer cells. All experiments were repeated four times. The experimental approach is outlined in the graphical abstract, Fig 1. The purity of MOs was verified by direct immunofluorescence (S1 Fig).

2. Specimen samples. Primary tumor tissue specimens and autologous peripheral blood samples were collected thanks to three patient volunteers, admitted to the Surgery Department of Tlemcen Medical Centre University (Algeria), who have been newly diagnosed for human epidermal growth factor receptor 2-Positive/estrogen receptor-Negative/progesterone receptor-Negative (ER⁻/PR⁻/HER2⁺) breast cancer (age group 50–60 years), and who have not yet begun treatment, after obtaining informed and written consent from each to participate to the current study. Peripheral blood was collected in heparinized *Vacutainer* tubes (BD, Bellingham Industrial Estate, UK). The homogeneity of sample biopsies and absence of intertumor variations for each tumor intended for experimental analyses were checked by macroscopical and thorough anatomopathological examinations, and based on cellular morphology and immunohistochemical analyses. All tumor samples are grade 2 nonspecific invasive mammary carcinoma classified as pT2N0. The current study was approved by local Ethics Committee of Tlemcen University, in accordance with the Declaration of Helsinki.

3. Isolation of mammary adherent tumor epithelial cells. After removal of the healthy tissue surrounding the tumor tissue, tumor mammary epithelial cells presenting as infiltrating ductal carcinomas were isolated from primary cancer specimens by enzymatic digestion and differential centrifugation according to Feller *et al.*, and Speirs *et al.* [22,23], with some modifications. Briefly, the tumor tissue specimens were washed extensively with 1x phosphate saline buffer (PBS), placed in sterile Petri dishes and cut into small 2 mm pieces with a sterile scalpel. The minced tissue was incubated in 0.1% collagenase solution at 37°C for 12–20 h. Following digestion, cell mixtures were centrifuged at 40 x g for 1 min and the supernatant transferred to new tubes that were then centrifuged at 100 x g for 2 min to obtain a pellet representing tumor epithelial cells.

4. Cell culture. Epithelial cancer cells were washed with RPMI-1640 medium, supplemented with 10% fetal calf serum (FCS) and 50 μ g/mL gentamicin, by centrifugation at 40 x g

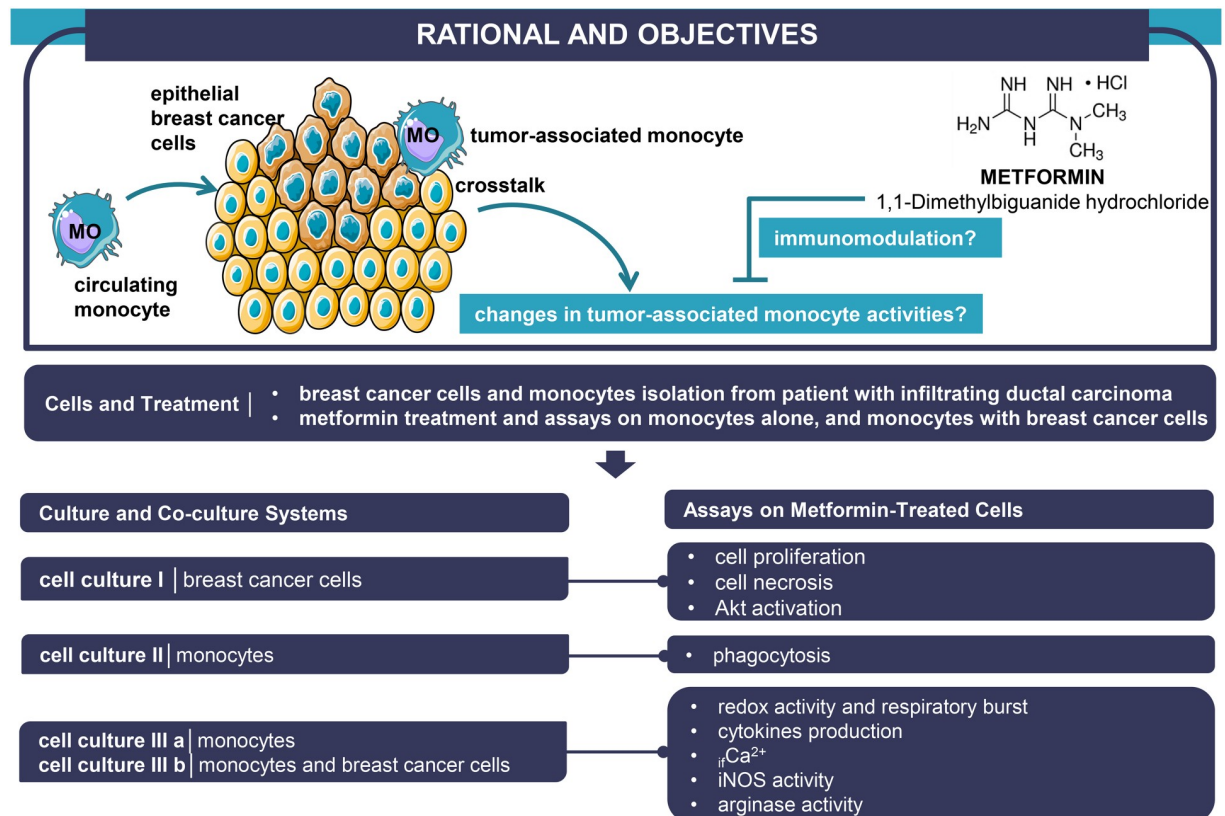


Fig 1. Summary of experimental design. Akt: protein kinase B (PKB), $_{i}Ca^{2+}$: intracellular free calcium ions, iNOS: nitric oxide synthase, MO: monocyte.

<https://doi.org/10.1371/journal.pone.0240982.g001>

for 5 min. The cell pellet was resuspended with 10 mL of RPMI-1640 supplemented with 10% FCS and 50 μ g/mL gentamicin and then subdivided into two culture flasks and incubated in a humidified atmosphere at 37°C and 5% CO₂. Fibroblast contamination was removed from epithelial cancer cells by differential trypsinization [24]. The culture medium was changed every 2–5 days [25]. Cells were passaged with 0.25% trypsin-EDTA (ethylenediamine tetraacetic acid) when they reached ~80% confluence [26].

5. Peripheral blood mononuclear cells isolation. Blood samples were diluted 1:1 with PBS and layered on Histopaque-1077 (Sigma-Aldrich, St. Louis MO, USA) and centrifuged at 400 x g for 30 min. The interface band containing PBMCs was carefully harvested washed twice with PBS. Cell pellets were suspended in 1 mL of RPMI-1640 supplemented with 10% FCS and 50 μ g/mL of gentamicin for cell counting. Cell viability was performed by TBET using photonic microscopy (Zeiss, Germany).

6. MOs isolation. MOs were isolated from PBMCs based on differential plastic adherence [27]. Briefly, PBMCs were cultivated in RPMI-1640 supplemented with 10% FCS and 50 μ g/mL gentamicin, and seeded at 2 x 10⁶ cell/mL into 24-well plates. Cells were allowed to adhere for 2 h at 37°C before removal of non-adherent cells were and treatment of adherent MOs with MET. Cells were counted microscopically (Zeiss, Germany) using trypan blue staining, and the purity of monocytes was evaluated by fluorescent staining with PhycoErytherin (PE)-anti-human CD14 antibody (BD Biosciences, San Diego, CA, USA) using a Floid Cell Imaging

Station (Thermo Fisher Scientific, MA USA) [28,29] and routinely exceeded over 90% purity (S1 Fig).

7. Cell culture and co-culture systems. After cell detachment with trypsin-EDTA [30], breast cancer cells were counted before being cultured alone or co-cultured with an equal number of MOs (2×10^5 cells/mL) at a ratio of 1:1 in RPMI-1640 supplemented with 10% FCS and 50 $\mu\text{g}/\text{mL}$ gentamicin.

8. MET treatment. MOs, breast cancer cells or co-cultured MOs with breast cancer cells were treated for 24 h with fresh medium containing or not MET at the dose of 2.5 mM [15].

9. TBET assays. The effect of MET treatment on cancer cell viability was based on TBET. Breast cancer cells (2×10^5 cells per well) were grown overnight in a 24-well plate at 37°C in a humidified atmosphere and 5% CO₂ for adherence. Thereafter, culture medium was replaced with fresh RPMI-1640 medium containing MET and incubated a further 24 h. Cells were subsequently washed with 1x PBS, trypsinized before determination the number of viable and dead cells with TBET.

10. BrdU assays. Cell proliferation was measured by BrdU incorporation using a BrdU Cell Proliferation ELISA according to the manufacturer's instructions (ab126556-BrdU Cell Proliferation kit, Abcam, Germany). Briefly, breast cancer cells (2×10^5 cells/mL) were treated with MET in 96-well microplates for 24 h at 37°C in a humidified atmosphere and 5% CO₂. Thereafter, 20 μL of the diluted 1x BrdU was added to each well and cells were incubated overnight. Cells were then fixed and BrdU incorporation detected using anti-BrdU monoclonal Detector Antibody for 1 h at room temperature before incubation with peroxidase goat anti-mouse IgG conjugate as secondary antibody. Color was developed using tetramethylbenzidine (TMB) as a peroxidase substrate and BrdU incorporation measured at 450 nm using an ELISA reader (Biochrom Anthos 2020, Cambridge, UK).

11. Western blotting assays. After 24 h incubation of breast cancer cells treated or not with MET, cells were washed with PBS and lysed using Triton X-100. Proteins present in equal amounts of cell lysates were rapidly diluted with SDS-sample buffer (50 mM Tris-HCl pH 6.8, 2 mM DTT, 1.0% SDS), boiled for 5 min. Proteins were separated by 10% sodium dodecyl-sulfate polyacrylamide gel electrophoresis (SDS-PAGE). Protein concentrations were not determined before reduction and denaturation to minimize the chance of protein dephosphorylation. After separation, proteins were transferred to a nitrocellulose membranes and transferred protein were visualized by staining with Ponceau red. Thereafter, membranes were blocked with 5% nonfat milk or 5% bovine serum albumin (BSA) for 45 min at room temperature and incubated overnight at 4°C with primary antibodies against p-Akt (Ser473) (1/1000), Akt-1 (2H10) (1/1000), Akt-2 (5B5) (1/1000) Cell Signaling Technology (Denvers, MA, USA). Horseradish peroxidase-conjugated (HRP) anti-mouse IgG and anti-rabbit IgG were used as secondary antibodies for 1 h at room temperature. Blotted membranes were detected with enhanced chemiluminescence reagent (Amersham Pico) using X-ray film. Quantitative analysis of the signals from scanned films was performed using *Imgcalc2*, a unix software developed in house (IGH, Montpellier) for quantifying pixels on numerical images. The results in Fig 2 are represented as a ratio to the signal in Ponceau Red staining to correct for differences in total protein loading with the levels for MET at dose 0 set as 1.

12. Phagocytosis assay. Assay for phagocytosis capacity was performed as described [31–33]. Briefly, a total of 2×10^5 MOs were infected with *Staphylococcus aureus* at multiplicity of infection (MOI) of 50 in a 24-well plate and incubated with MET for 1 h at 37°C in a 5% CO₂ incubator. The number of viable bacteria was determined by serial dilution and colony forming unit (CFU) counts on Chapman medium. The percentage of phagocytosis was calculated

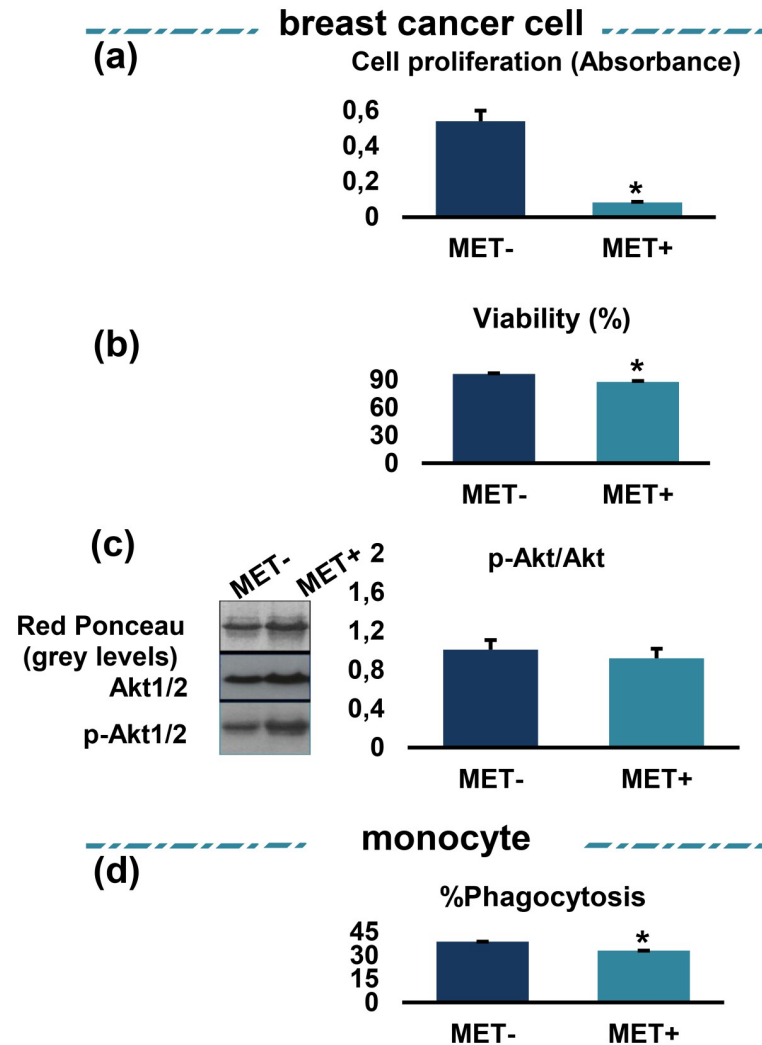


Fig 2. Effect of MET treatment on breast cancer cell proliferation, viability, ratio of phosphorylated Akt-to-total Akt and MOs phagocytosis capacity. In breast cancer cells treated or not with MET, (a) cell proliferation was determined by BrdU assay and (b) viability by TBET assay. (c) phosphoAkt to Akt ratio: levels of major proteins stained by red Ponceau are shown as loading control. Values are represented as a ratio to the protein levels in Ponceau red and with the value for zero MET set as 1. MET: metformin, p-Akt: phosphorylated Akt. (d) MOs were infected with *Staphylococcus aureus* before treatment with MET. The results were expressed as a percentage of phagocytosis. Values are presented as the mean with standard error of mean for four independent experiments carried out on three samples (n = 12 for each group). Asterisks indicate significant differences between treated cells and untreated controls by Mann-Whitney U test (*p < 0.05). MET: metformin, MOs: monocytes.

<https://doi.org/10.1371/journal.pone.0240982.g002>

as follows:

$$\text{Phagocytosis\%} = M_{t_0} - 100 \times \frac{\left(\frac{NEC}{NC_1/NC_0} \right)}{M_{t_0}}$$

M_{t_0} is the number of bacteria in the assay sample mixture at t_0 . NEC, number of extracellular bacteria in assay mixtures sample at t_1 . NC_0 and NC_1 correspond to control sample at t_0 and t_1 .

13. Arginase activity assay. The enzymatic activity of arginase (EC 3.5.3.1) was evaluated in cell lysates based on determination of urea levels following the L-arginine hydrolysis as described in detail [34]. The arginase activity was expressed as mU urea/mg protein/1 h.

14. iNOS activity assay. Measurement of iNOS activity was based on the determination of NO generation levels. The accumulation of NO in cell-free culture supernatants were evaluated by nitrite (NO₂) measurement, as stable and final end-product of NO, using a sensitive colorimetric Griess reaction as described in detail [34,35]. Absorbance was measured at 540 nm using a Biochrom Anthos 2020 ELISA plate reader. NO production levels were calculated by comparison with a sodium nitrite (NaNO₂) curve standard [36]. iNOS activity was obtained by normalizing each NO concentration to milligrams of protein and expressed as picomoles/mg protein/30 min.

15. LDH-based cytotoxicity assays. LDH-based cytotoxicity levels were determined by evaluation of LDH release into the cell culture supernatants using Lactate Dehydrogenase Activity Assay kit (MAK066, Sigma-Aldrich). Briefly, 50 μL of supernatant and 50 μL of the Master Reaction Mix were mixed and added to each well of a 96-well plate. Absorbance was measured at 450 nm after 30 min incubation at 37°C in accordance with the manufacturer's instructions.

16. ${}_{i\text{f}}\text{Ca}^{2+}$ assay. The concentrations of ${}_{i\text{f}}\text{Ca}^{2+}$ were measured biochemically based on the ortho-cresolphthalein complexone (oCPC) method as described elsewhere [37].

17. Cytokine assays. Concentration of IFN-γ and IL-10 in cell culture media of MOs or co-culture system supernatants were measured by sandwich enzyme-linked immunosorbent assays (ELISA), using respective commercial kits (BD Biosciences), according to the manufacturer's instructions. Optical densities (OD) were measured at 450 nm using appropriate standard curves for each cytokine.

18. Protective redox activity assays. Redox activity was evaluated by determination of the levels of catalase and SOD activities.

18.1. Catalase activity assay. The enzymatic activity of catalase was spectrophotometrically determined in cell lysates by measurement of hydrogen peroxide (H₂O₂) decomposition [38]. 10 μL volumes of cell lysates were added to a reaction mixture of H₂O₂ in 0.9% (v/v) aqueous saline before incubation for 5 min. The reactions were stopped by the addition of Titanyl sulfate (TiOSO₄), and the absorbance measured at 410 nm.

18.2. SOD activity assay. SOD activity in cell lysates was determined spectrophotometrically by measuring production of a water-soluble formazan dye resulting from the reduction of Dojindo's highly water-soluble tetrazolium salt WST-1 ((2-4-Iodophenyl)-3-(4-nitrophenyl)-5-(2,4-disulfophenyl)-2H-tetrazolium, monosodium salt), using a SOD Assay Kit-WST (19160, Sigma Aldrich). Twenty μL of the enzyme working solution were added to a mixture containing 20 μL of cell lysate and 200 μL of WST Working Solution. The microplate was incubated at 37°C for 20 min, and the absorbance read at 440 nm. The SOD activity (percentage inhibition of WST-1 inhibition) was calculated as follows:

$$\text{SOD activity (inhibition rate \%)} = \frac{(\text{Ablank1} - \text{Ablank3}) - (\text{Asample} - \text{Ablank2})}{(\text{Ablank1} - \text{Ablank3})} \times 100$$

19. Statistical analysis. Data are presented as the mean with standard errors of means (SEM). Statistical analyses were performed using non-parametric Mann-Whitney *U* or Kruskal-Wallis one-way analysis of variance (ANOVA) test with pairwise comparisons using the Dunn-Bonferroni approach after checking the distribution of data. Statistics were carried out using IBM SPSS Statistics version 20. *P*-values less than 0.05 were considered significant.

Results

1. MET effects on breast cancer cells and on monocytes cultured alone

1.1. MET downregulates breast cancer cell viability and proliferation, while has no effect on the ratio of phosphorylated Akt1/2 versus total Akt1/2. As shown in Fig 2a and 2b, MET treatment significantly downregulated breast cancer cell proliferation and viability levels (for both comparisons, $p < 0.05$). Fig 2c shows the raw data of the actual protein levels (upper panels), total Akt1/2 levels (middle panels) and levels of phospho-(activated) Akt1/2 (lower panels). The histogram shows the relative expression levels of activated Akt1/2-to-total Akt1/2 ratio after normalization to the total protein loaded. As observed in Fig 2c, MET treatment did not show a significant difference in either Akt levels and ratio of activated Akt versus total Akt when comparing with MET-untreated cells ($p > 0.05$). So the actions of MET on Akt1/2 are essentially due to a loss/reduction of Akt1/2 activity since when the ratio of active Akt1/2 (phosphorylated) to total Akt1/2 levels is calculated we observed a reduction of Akt1/2 activity in cancer cells.

1.2. MET downregulates monocyte phagocytosis. As shown in Fig 2d, the phagocytic activity of MOs significantly decreased after MET treatment ($p < 0.05$).

2. MET effects on MO cells in monoculture and co-culture systems

2.1. MET might reverse the co-culture effect on LDH-based cytotoxicity levels, but has no cytotoxic effect on MOs cultured alone. As shown in Fig 3, MET treatment induced no necrosis/LDH-based cytotoxicity effects on MO cells ($p > 0.05$). Additionally, MET might reverse the co-culture effect on LDH-based cytotoxicity levels. Conversely, the level of LDH-based cytotoxicity was significantly downregulated in MET-untreated co-cultures of MOs with breast cancer cells when compared to MET-untreated MOs cultured alone ($p < 0.05$).

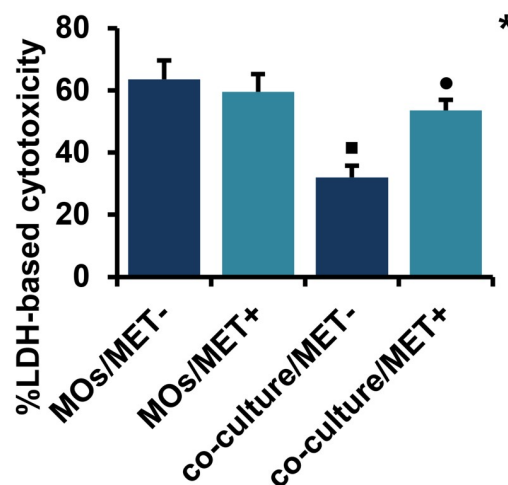


Fig 3. Cytotoxic effect of MET on MOs and co-culture system. Necrosis levels were measured spectrophotometrically through the evaluation of LDH release. Values are presented as the mean with standard error of mean for four independent experiments carried out on three samples ($n = 12$ for each group). MET: metformin, LDH: lactate dehydrogenase, MOs: monocytes, MOs/MET⁻: MET-untreated MOs, MOs/MET⁺: MET-treated MOs, co-culture/MET⁻: MET-untreated co-culture system, co-culture/MET⁺: MET-treated co-culture system. Black dots indicate significant differences when comparing each treated group with untreated controls (0 mM MET) using Mann-Whitney U test ($*p < 0.05$). Black boxes indicate significant differences highlighted between MET-untreated MOs and MET-untreated co-culture system using Mann-Whitney U test ($*p < 0.05$). Asterisks indicate significant differences highlighted between all groups by Kruskal-Wallis test with pairwise Dunn-Bonferroni adjustment ($*p < 0.05$).

<https://doi.org/10.1371/journal.pone.0240982.g003>

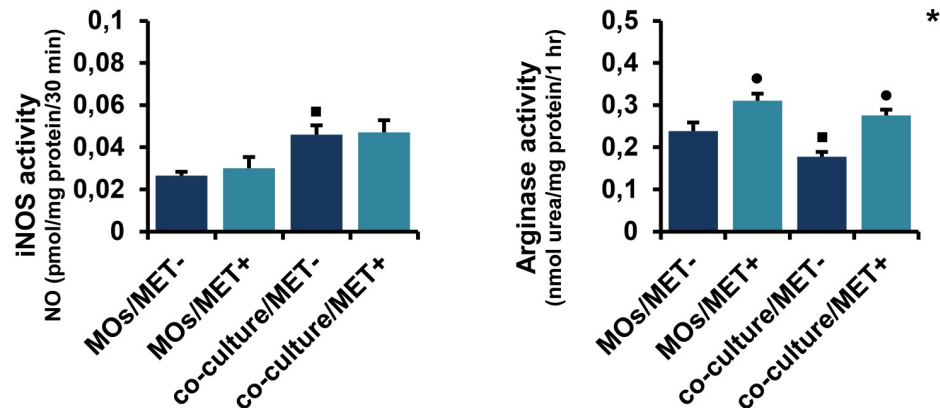


Fig 4. Effect of MET on iNOS and arginase activities in MOs and co-culture system. NO levels were measured by Griess colorimetric reaction and iNOS activity was obtained by normalizing each NO to protein concentrations and time. The enzymatic activity of arginase was evaluated in cell lysates by the spectrophotometric measurement of urea concentration. Values are presented as the mean with standard error of mean for four independent experiments carried out on three samples ($n = 12$ for each group). MET: metformin, MOs: monocytes, NO: nitric oxide, iNOS: inducible nitric oxide synthase, MOs/MET⁻: MET-untreated MOs, MOs/MET⁺: MET-treated MOs, co-culture/MET⁻: MET-untreated co-culture system, co-culture/MET⁺: MET-treated co-culture system. Black dots indicate significant differences when comparing each treated group with untreated controls (0 mM MET) using Mann-Whitney U test ($*p < 0.05$). Black boxes indicate significant differences highlighted between MET-untreated MOs and MET-untreated co-culture system using Mann-Whitney U test ($*p < 0.05$). Asterisks indicate significant differences highlighted between all groups by Kruskal-Wallis test with pairwise Dunn-Bonferroni adjustment ($*p < 0.05$).

<https://doi.org/10.1371/journal.pone.0240982.g004>

2.2. MET ameliorates simultaneously iNOS and arginase activities in co-cultures of MOs with breast cancer cells. As depicted in Fig 4, MET induced an increase in iNOS activity in co-culture systems, as compared to MET-treated or MET-untreated MOs cultured alone; while the difference was not significant for the comparison with MET-treated MOs (respectively, $p > 0.05$ and $p < 0.05$). Additionally, iNOS activity was significantly upregulated in MET-untreated MOs co-cultured with breast cancer cells in comparison to MET-untreated MOs cultured alone ($p < 0.05$). Similarly, (Fig 4), MET might improve the co-culture effect on arginase activity and significantly increased the arginase activity of MOs cultured alone ($p < 0.05$). However, arginase activity was significantly downregulated in MET-untreated MOs co-cultured with breast cancer cells compared to MET-untreated MOs cultured alone ($p < 0.05$).

2.3. MET reverses the co-culture effect on catalase activity, but not on SOD activity. As demonstrated in Fig 5, MET had no significant effect on catalase activity in MO cells while might reverse the co-culture effect on catalase activity. Additionally, catalase activity was significantly downregulated in MET-untreated co-cultures of MOs with breast cancer cells than in MET-untreated MOs cultured alone ($p < 0.05$). Moreover, SOD activity was strongly increased in MET-treated compared to MET-untreated MOs ($p < 0.05$). In contrast to MOs cultured alone, MET had no significant effect on SOD activity in co-culture systems.

2.4. The effects of MET on $_{iF}Ca^{2+}$ differs between MOs cultured alone and MOs co-cultured with breast cancer cells. As shown in Fig 6, MET had no significant effect on $_{iF}Ca^{2+}$ levels in MO cells while might reverse the co-culture effect on $_{iF}Ca^{2+}$ levels ($p < 0.05$). Conversely, MET treatment downregulated $_{iF}Ca^{2+}$ in MET-untreated MOs co-cultivated with breast cancer cells more significantly than in MET-untreated MOs cultured alone ($p < 0.05$).

2.5. MET reverse the effect of co-culture on the production of IFN- γ and IL-10. As shown in Fig 7, MET induced a significant upregulation of IFN- γ levels and a significant downregulation of IL-10 levels in MOs cultured alone (for the two comparisons, $p < 0.05$).

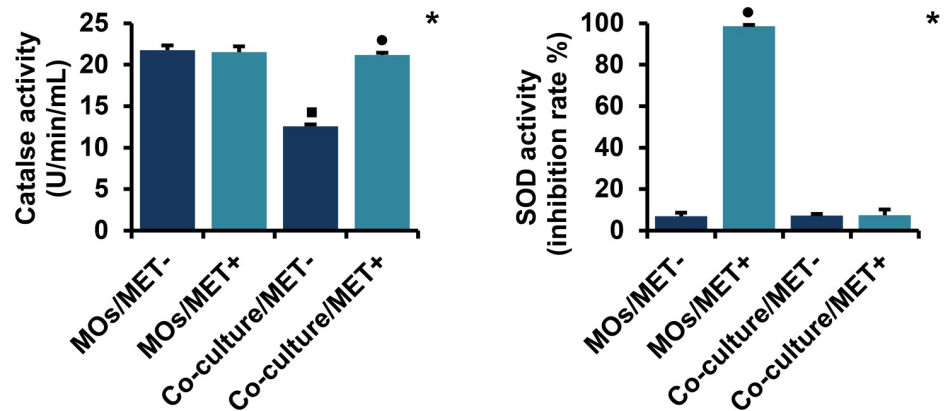


Fig 5. Effect of MET on catalase and SOD activities in MOs and co-culture system. Catalase activity was determined spectrophotometrically by measurement of hydrogen peroxide decomposition. SOD activity was evaluated by spectrophotometric measurement of a water-soluble formazan dye. Values are presented as the mean with standard error of mean for four independent experiments carried out on three samples ($n = 12$ for each group). MET: metformin, MOs: monocytes, SOD: superoxide dismutase, MOs/MET⁻: MET-untreated MOs, MOs/MET⁺: MET-treated MOs, co-culture/MET⁻: MET-untreated co-culture system, co-culture/MET⁺: MET-treated co-culture system. Black dots indicate significant differences when comparing each treated group with untreated controls (0 mM MET) using Mann-Whitney U test ($*p < 0.05$). Black boxes indicate significant differences highlighted between MET-untreated MOs and MET-untreated co-culture system using Mann-Whitney U test ($*p < 0.05$). Asterisks indicate significant differences highlighted between all groups by Kruskal-Wallis test with pairwise Dunn-Bonferroni adjustment ($*p < 0.05$).

<https://doi.org/10.1371/journal.pone.0240982.g005>

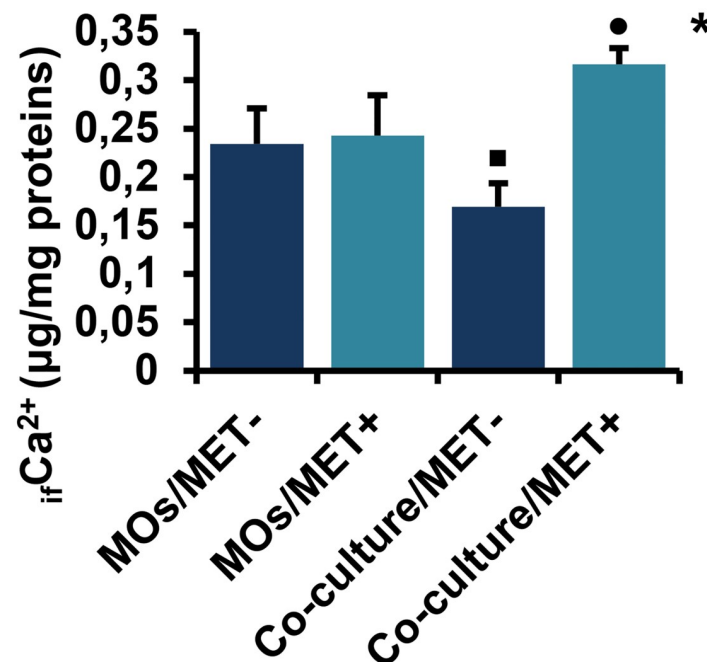


Fig 6. Effect of MET on iCa^{2+} levels in MOs and co-culture system. Values are presented as the mean with standard error of mean for four independent experiments carried out on three samples ($n = 12$ for each group). MET: metformin, MOs: monocytes, iCa^{2+} : intracellular free calcium ions, MOs/MET⁻: MET-untreated MOs, MOs/MET⁺: MET-treated MOs, co-culture/MET⁻: MET-untreated co-culture system, co-culture/MET⁺: MET-treated co-culture system. Black dots indicate significant differences when comparing each treated group with untreated controls (0 mM MET) using Mann-Whitney U test ($*p < 0.05$). Black boxes indicate significant differences highlighted between MET-untreated MOs and MET-untreated co-culture system using Mann-Whitney U test ($*p < 0.05$). Asterisks indicate significant differences highlighted between all groups by Kruskal-Wallis test with pairwise Dunn-Bonferroni adjustment ($*p < 0.05$).

<https://doi.org/10.1371/journal.pone.0240982.g006>

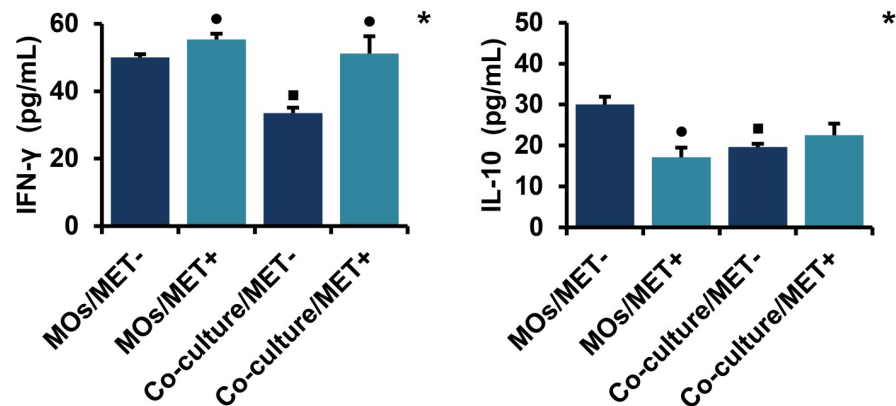


Fig 7. Effect of MET on the production of IL-10 and IFN- γ in MOs and co-culture system. IL-10 and IFN- γ levels were measured using sandwich enzyme-linked immunosorbent assay (ELISA). Values are presented as the mean with standard error of mean for four independent experiments carried out on three samples ($n = 12$ for each group). MET: metformin, MOs: monocytes, IFN: interferon, IL: interleukin, MOs/MET⁻: MET-untreated MOs, MOs/MET⁺: MET-treated MOs, co-culture/MET⁻: MET-untreated co-culture system, co-culture/MET⁺: MET-treated co-culture system. Black dots indicate significant differences when comparing each treated group with untreated controls (0 mM MET) using Mann-Whitney U test ($\bullet p < 0.05$). Black boxes indicate significant differences highlighted between MET-untreated MOs and MET-untreated co-culture system using Mann-Whitney U test ($\blacksquare p < 0.05$). Asterisks indicate significant differences highlighted between all groups by Kruskal-Wallis test with pairwise Dunn-Bonferroni adjustment ($*p < 0.05$).

<https://doi.org/10.1371/journal.pone.0240982.g007>

Additionally, co-culture induced a significant downregulation of both IFN- γ and IL-10 levels ($p < 0.05$), which are reversed after MET treatment.

Discussion

MET has recently received increasing attention as a potential therapeutic treatment against cancer [39]. Here we have examined the effects of MET in a novel co-culture system comprising primary MOs and ER⁻/PR⁻/HER2⁺ breast cancer cells.

Breast tumors characterized by overexpression of HER2 have been correlated with increased tumor aggressiveness, invasiveness and poorer prognosis [40]. Measuring several different biomarkers of phenotypic functional activities of MOs before and during their interplay with primary ER⁻/PR⁻/HER2⁺ breast cancer cells, we confirm scientific relevance of the co-culture system over the use of isolated cell types for analyzing the reversing effects of MET in a tumor-like microenvironment, where cancer cells usually alter immune cell functions, especially affecting their cell metabolism and ability for the production of antitumor cytokines, like co-operative cytokines IFN- γ and IL-10.

The dose of MET used in these experiments (2.5 mM) is relatively higher than those used clinically for the treatment of type 2 diabetes (ca 0.5 mM). However, it is important to note that *in vitro* cultured cells are maintained under less physiological conditions. In particular, cultured cells do not benefit from the indirect anti-tumor effects of MET occurring *in vivo* such as the reduction of insulin levels—where insulin is known to have a mitogenic effect—and cultured cells are exposed to high concentrations of growth factors and glucose present in the culture medium, which may help explain the required higher doses of MET [41].

The anti-tumorigenic properties of MET have been reported in several studies associated with indirect action (reduced insulin levels) or direct actions on molecular pathways that regulate breast tumor cell growth and death [42]. MET may mediate its effects through actions on different cells of the tumor microenvironment, including MOs-macrophages that would be involved in controlling tumor cell growth and progression. However, the activities of immune

cells could undoubtedly change when they are in contact with tumor cells. In this context, we investigated the effect of MET on functional activities of autologous MOs cultured alone and when co-cultured with primary breast cancer cells. In conclusion, our results demonstrate a significant effect of MET during MOs-breast cancer cells crosstalk.

Here, we first tested the effects of MET on proliferation and viability of cancer cells. We found that MET downregulated both the proliferation and viability of breast cancer cells. Our results are consistent with those obtained recently using BrdU and 3-(4,5-Dimethylthiazol-2-yl)-2,5-diphenyltetrazolium bromide for (MTT) assays on breast cancer cell lines MCF-7, MDA-MB-231 and MDA-MB-435 [17,43]. The same effects were observed on MCF-7 and MDA-MB-231 cell viability with the doses of at 1 mM and 5 mM of MET using TBET assays after 24 h and 48 h of treatment [44]. In terms of cell activation and proliferation, the PI3K/Akt/mTOR signaling pathway has been highlighted to play an important role in vital cell functions including cell growth, proliferation, differentiation and survival [45]. Its hyper-activation can lead to excessive tumor cell proliferation, inhibition of apoptosis, angiogenesis, invasion and metastasis [46–48]. For our part, at the concentration of MET used (2.5 mM) we found a modest and non significant reduction of the PI3K/Akt activation in breast cancer cells. However, several studies reported that metformin reduced the survival and proliferation rate of breast cancer cells through the inhibition of PI3K/Akt signaling pathway [49,50].

The phagocytic activity of MOs is the subject of several studies under normal and pathological conditions, including breast cancer [51]. In our study, we observed that pretreatment with MET downregulated the phagocytic capacity of MOs, which is of interest, knowing that high phagocytic capacity is associated with MOs that promote survival and extravasation of cancer cells, and characterizes the so-called 'classical MOs' in humans [52,53].

Measuring levels of proliferation and phagocytosis in co-culture systems was uninformative because BrdU incorporation and anti-Akt antibodies used for viability and proliferation assays do not discriminate for one cell type or the other in the co-culture [54–56] and the bacteria used for phagocytosis assay have the ability to invade and replicate within several types of phagocytic and nonphagocytic cells, including epithelial cells and this invasion can lead to apoptosis [10,57].

It is well known that necrosis and iNOS are both involved in tissue damage occurring during inflammation. Our results showed that MET treatment had no effect on MOs necrotic death as demonstrated by LDH-based cytotoxicity. However, MET might ameliorate the co-culture effect on necrosis, which is in agreement with previous *in vitro* studies, carried out on BT-20 breast cancer cell line [18]. In MOs, as well as in other cells especially macrophages, the amino acid L-arginine is also used as a substrate by arginase to produce polyamines [58] that contribute to the tumor progression [59], and by iNOS to produce NO [58], which has antitumor effects at high levels [60]. The current study provides evidence that MOs cultured with breast cancer cells exhibited high levels of iNOS, but remain without marked change when treated with MET. Our observations are in agreement with earlier findings demonstrating that MET induces antitumoral activity of macrophages during breast cancer [61] and suppresses polarization toward pro-tumoral phenotypes [62]. Although arginase activity was downregulated in untreated co-cultured cells, it was reversed after MET treatment. Hence, MET has been reported to have opposing effects in normal or pathological conditions whereby it can both attenuate NO production and enhance arginase activation in MOs and macrophages [63,64]. It would be of interest to check the impact of MET treatment on iNOS and arginase activities simultaneously.

The link between cancer and altered metabolism has previously been suggested as a common feature of cancerous tissues, such as the Warburg effect, in which some antioxidant molecules can be used in protective mechanisms against oxidative stress and ROS that are

produced during rapid cell proliferation [65]. High levels of ROS can cause macromolecular damage, that can lead to apoptosis and senescence [66]. Our findings demonstrated that catalase activity was downregulated in MET-untreated co-cultures, whereas the co-culture effect on catalase activity can be reversed by MET treatment. Additionally, SOD activity was changed only in MET-treated MOs. In summary, MET treatment did not show metabolic alterations with regard to the levels of the antioxidant molecules catalase and SOD within the co-cultures of MOs with breast cancer cells compared to MOs cultivated alone.

$_{i}Ca^{2+}$ is an important secondary messenger that regulates various cellular processes and signaling pathways including those related to cancer, such as apoptosis, proliferation and metastasis [67,68], and those involved in immune responses of MOs, including the production of cytokines and phagocytic activation [69,70]. We first observed that $_{i}Ca^{2+}$ levels were reduced in co-culture of MOs with breast cancer cells. In contrast, MET treatment induced $_{i}Ca^{2+}$ upregulation in MOs and might reverse the effect of co-culture. So, it has been reported that increased levels of calcium ions are related to both MO activation and the induction of apoptosis in breast cancer cells [68,71,72].

It is now accepted that IL-10 enhances cancer immune surveillance and suppression of cancer-associated inflammation [73], as well as inducing expression of IFN- γ [74], which exerts antitumor activities directly by enhancement of tumor cells antigenicity, inhibition of cell proliferation, the induction of apoptosis or indirectly by inhibition of angiogenesis [75]. Our results indicate that the levels of both IL-10 and IFN- γ decreased during interplay between MOs and breast cancer cells. Except with IL-10, treatment with MET has shown marked differences between its action when MOs are cultured alone and when co-cultured with breast cancer cells. MET induced a decrease in IL-10 levels in MOs and, conversely, an increase in IFN- γ levels. However, MET treatment might ameliorate the co-culture effect on the production of both cytokines, although the differences were not significant for IL-10. So, the results did not show significant differences for IL-10 between cultures of MOs alone, in the absence of treatment, and cultures of MOs with breast cancer cells, treated with MET. These suggest that MET could contribute to the conservation of IL-10 expression levels when MO comes into contact with cancer cells, without inducing changes usually seen after interplay with cancer cells. Our results demonstrate that MET treatment is clearly effective and important in a system that shares some similarities with the biological system where mononuclear cells are not alone but may be confronted with malignant cells.

Of note, circulating MOs can exert different roles based on phenotype characterization. Hence, it has been reported that circulating monocytes subsets so-called classical inflammatory monocytes (moM1, CD14⁺⁺/CD16⁻) and patrolling non-classical monocytes (moM3, CD14⁺/CD16⁺⁺) exert opposite effects after their recruitment in tumor microenvironment *via* the chemokine (C-C motif) ligand 2 (CCL2), also referred to as monocyte chemoattractant protein 1 (MCP1) and small inducible cytokine A2, which is secreted by malignant cells. moM1 can be recruited to the tumor microenvironment where they can be transformed into tumor-associated macrophages (TAMs) that facilitate tumorigenesis by suppression of CD8⁺ T-cell function, recruitment of regulatory T (Treg) cells, angiogenesis, tumor cell intravasation, and metastasis [76], while moM3 display an anti-tumoral role, by directly engulfing cancer cells and by releasing CCL3, CCL4 and CCL5 chemokines, which in turn induce recruitment and activation of cytotoxic natural killer (NK) cells [52]. Another subset of circulating and tumor-associated monocytes endowed with proangiogenic activity, are characterized by the expression of the TIE-2/Tek angiopoietin receptor, Endoglin and VEGF-R2 in the intermediate monocytes subset (moM2, CD14⁺⁺/CD16⁺) as confirmed by a genomic analysis [77]. TIE-2 expressing monocytes (TEM) are recruited to the tumor site where they have been shown to be essential for angiogenesis and inhibition of tumor cell apoptosis by mechanisms depending

on TNF- α release. They also have the highest capacity to induce CD4⁺ T-cell activation [78]. Therefore, it would be of interest to investigate MET effects on all characterized MO subsets before and after their individual crosstalk with the studied autologous breast cancer cells. The specific objective being to see whether or not MET treatment would reverse the pro-tumoral activities of moM1 and moM2, knowing that monocytes are endowed with plasticity and versatility in their phenotype [79,80].

Conclusions and future prospects

In fine, our results not only show that the activities of human MOs change when they interact with autologous primary breast cancer cells, but also provide the first evidence that MET treatment can have a potent role in reversing the effects of the crosstalk between MOs and breast cancer cells, especially on the production of co-operative ‘antitumor IFN- γ ’ and ‘regulatory IL-10’ cytokines, intracellular calcium signals, as well as immune-metabolic and protective redox based-biomarkers as summarized in the graphical abstract (S2 Fig). These findings open the route to further investigations including the study of MET on autophagy/reverse Warburg effects, as well as the molecular characterization of different subsets of monocytes involved in the interaction with breast cancer cells following MET treatment.

Supporting information

S1 Fig.

(DOCX)

S2 Fig.

(DOCX)

S3 Fig.

(PDF)

Acknowledgments

The authors are grateful to the Team W0414101 of the Laboratory of Applied Molecular Biology and Immunology (University of Tlemcen, Algeria) for their help and technical assistance.

Author Contributions

Conceptualization: Zoheir Dahmani, Gérard Lefranc, Ned J. Lamb, Mourad Aribi.

Data curation: Zoheir Dahmani, Lynda Addou-Klouche, Aida Messaoud, Mahmoud Idris Benaissti, Hadjer Terbeche, Marwa Miliani, Anne Fernandez.

Formal analysis: Zoheir Dahmani, Sara Dahou, Nihel Chahinez Djebri, Wafa Nouari, Anne Fernandez, Ned J. Lamb, Mourad Aribi.

Funding acquisition: Mourad Aribi.

Investigation: Zoheir Dahmani, Lynda Addou-Klouche, Florence Gizard, Sara Dahou, Aida Messaoud, Nihel Chahinez Djebri, Mahmoud Idris Benaissti, Wafa Nouari, Marwa Miliani, Gérard Lefranc, Anne Fernandez, Mourad Aribi.

Methodology: Zoheir Dahmani, Florence Gizard, Mahmoud Idris Benaissti, Meriem Mostefaoui, Hadjer Terbeche, Wafa Nouari, Marwa Miliani, Anne Fernandez, Ned J. Lamb, Mourad Aribi.

Project administration: Gérard Lefranc, Mourad Aribi.

Software: Ned J. Lamb.

Supervision: Florence Gizard, Gérard Lefranc, Anne Fernandez, Ned J. Lamb, Mourad Aribi.

Validation: Zoheir Dahmani, Sara Dahou, Aida Messaoud, Nihel Chahinez Djebri, Mahmoud Idris Benaissi, Meriem Mostefaoui, Hadjer Terbeche, Mourad Aribi.

Visualization: Zoheir Dahmani, Lynda Addou-Klouche, Florence Gizard, Sara Dahou.

Writing – original draft: Zoheir Dahmani, Ned J. Lamb, Mourad Aribi.

Writing – review & editing: Anne Fernandez, Ned J. Lamb, Mourad Aribi.

References

- Ghoncheh M, Pournamdar Z, Salehiniya H. Incidence and Mortality and Epidemiology of Breast Cancer in the World. *Asian Pac J Cancer Prev APJCP* (2016) 17:43–46.
- Soliman H. Immunotherapy strategies in the treatment of breast cancer. *Cancer Control J Moffitt Cancer Cent* (2013) 20:17–21.
- Gingras I, Azim HA, Ignatiadis M, Sotiriou C. Immunology and breast cancer: toward a new way of understanding breast cancer and developing novel therapeutic strategies. *Clin Adv Hematol Oncol HO* (2015) 13:372–382.
- Sabatier R, Finetti P, Mamessier E, Adelaide J, Chaffanet M, Ali HR, et al. Prognostic and predictive value of PDL1 expression in breast cancer. *Oncotarget* (2015) 6:5449–5464. <https://doi.org/10.18632/oncotarget.3216> PMID: 25669979
- Xu T, He B-S, Liu X-X, Hu X-X, Lin K, Pan Y-Q, et al. The Predictive and Prognostic Role of Stromal Tumor-infiltrating Lymphocytes in HER2-positive Breast Cancer with Trastuzumab-based Treatment: a Meta-analysis and Systematic Review. *J Cancer* (2017) 8:3838–3848. <https://doi.org/10.7150/jca.21051> PMID: 29151971
- Doseff A, Parihar A. “Monocyte Subsets and Their Role in Tumor Progression,” in *Tumor Microenvironment and Myelomonocytic Cells*, ed. Biswas S. (InTech). <https://doi.org/10.5772/32615>
- Ben-Baruch A. Host microenvironment in breast cancer development: Inflammatory cells, cytokines and chemokines in breast cancer progression: reciprocal tumor–microenvironment interactions. *Breast Cancer Res* (2002) 5: <https://doi.org/10.1186/bcr554> PMID: 12559043
- Evani SJ, Prabhu RG, Gnanaruban V, Finol EA, Ramasubramanian AK. Monocytes mediate metastatic breast tumor cell adhesion to endothelium under flow. *FASEB J* (2013) 27:3017–3029. <https://doi.org/10.1096/fj.12-224824> PMID: 23616566
- Mohamed M, Cavallo-Medved D, Rudy D, Anbalagan A, Moin K, Sloane B. Interleukin-6 Increases Expression and Secretion of Cathepsin B by Breast Tumor-Associated Monocytes. *Cell Physiol Biochem* (2010) 25:315–324. <https://doi.org/10.1159/000276564> PMID: 20110692
- Chiang C-F, Chao T-T, Su Y-F, Hsu C-C, Chien C-Y, Chiu K-C, et al. Metformin-treated cancer cells modulate macrophage polarization through AMPK-NF-κB signaling. *Oncotarget* (2017) 8: <https://doi.org/10.18632/oncotarget.14982> PMID: 28157701
- Stout RD, Suttles J. Functional plasticity of macrophages: reversible adaptation to changing microenvironments. *J Leukoc Biol* (2004) 76:509–513. <https://doi.org/10.1189/jlb.0504272> PMID: 15218057
- Idzkowska E, Eljaszewicz A, Miklasz P, Musial WJ, Tycinska AM, Moniuszko M. The Role of Different Monocyte Subsets in the Pathogenesis of Atherosclerosis and Acute Coronary Syndromes. *Scand J Immunol* (2015) 82:163–173. <https://doi.org/10.1111/sji.12314> PMID: 25997925
- Szaflarska A, Baj-Krzyworzeka M, Siedlar M, Węglarczyk K, Ruggiero I, Hajto B, et al. Antitumor response of CD14⁺/CD16⁺ monocyte subpopulation. *Exp Hematol* (2004) 32:748–755. <https://doi.org/10.1016/j.exphem.2004.05.027> PMID: 15308326
- Fan C, Wang Y, Liu Z, Sun Y, Wang X, Wei G, et al. Metformin exerts anticancer effects through the inhibition of the Sonic hedgehog signaling pathway in breast cancer. *Int J Mol Med* (2015) 36:204–214. <https://doi.org/10.3892/ijmm.2015.2217> PMID: 25999130
- Liu B, Fan Z, Edgerton SM, Yang X, Lind SE, Thor AD. Potent anti-proliferative effects of metformin on trastuzumab-resistant breast cancer cells via inhibition of erbB2/IGF-1 receptor interactions. *Cell Cycle* (2011) 10:2959–2966. <https://doi.org/10.4161/cc.10.17.16359> PMID: 21862872

16. Camacho L, Dasgupta A, Jiralerspong S. Metformin in breast cancer—an evolving mystery. *Breast Cancer Res* (2015) 17: <https://doi.org/10.1186/s13058-015-0598-8> PMID: 26111812
17. Queiroz EAIF, Puukila S, Eichler R, Sampaio SC, Forsyth HL, Lees SJ, et al. Metformin Induces Apoptosis and Cell Cycle Arrest Mediated by Oxidative Stress, AMPK and FOXO3a in MCF-7 Breast Cancer Cells. *PLoS ONE* (2014) 9:e98207. <https://doi.org/10.1371/journal.pone.0098207> PMID: 24858012
18. Ding L, Liang G, Yao Z, Zhang J, Liu R, Chen H, et al. Metformin prevents cancer metastasis by inhibiting M2-like polarization of tumor associated macrophages. *Oncotarget* (2015) 6: <https://doi.org/10.18632/oncotarget.5541> PMID: 26497364
19. O'Neill LAJ, Kishton RJ, Rathmell J. A guide to immunometabolism for immunologists. *Nat Rev Immunol* (2016) 16:553–565. <https://doi.org/10.1038/nri.2016.70> PMID: 27396447
20. Ferret P-J, Soum E, Negre O, Fradelizi D. Auto-protective redox buffering systems in stimulated macrophages. *BMC Immunol* (2002) 3:3. <https://doi.org/10.1186/1471-2172-3-3> PMID: 11914132
21. Yanagawa Y, Iwabuchi K, Onoé K. Co-operative action of interleukin-10 and interferon-gamma to regulate dendritic cell functions. *Immunology* (2009) 127:345–353. <https://doi.org/10.1111/j.1365-2567.2008.02986.x> PMID: 19191915
22. Feller WF, Stewart SE, Kantor J. Primary tissue culture explants of human breast cancer. *J Natl Cancer Inst* (1972) 48:1117–1120. PMID: 4336875
23. Speirs V, Green AR, Walton DS, Kerin MJ, Fox JN, Carleton PJ, et al. Short-term primary culture of epithelial cells derived from human breast tumours. *Br J Cancer* (1998) 78:1421–1429. <https://doi.org/10.1038/bjc.1998.702> PMID: 9836473
24. Jones JCR. Reduction of contamination of epithelial cultures by fibroblasts. *CSH Protoc* (2008) 2008: pdb.prot4478. <https://doi.org/10.1101/pdb.prot4478> PMID: 21356842
25. Farnie G, Clarke RB, Spence K, Pinnock N, Brennan K, Anderson NG, et al. Novel Cell Culture Technique for Primary Ductal Carcinoma In Situ: Role of Notch and Epidermal Growth Factor Receptor Signaling Pathways. *JNCI J Natl Cancer Inst* (2007) 99:616–627. <https://doi.org/10.1093/jnci/djk133> PMID: 17440163
26. Benton G, DeGray G, Kleinman HK, George J, Arnaoutova I. In Vitro Microtumors Provide a Physiologically Predictive Tool for Breast Cancer Therapeutic Screening. *PLOS ONE* (2015) 10:e0123312. <https://doi.org/10.1371/journal.pone.0123312> PMID: 25856378
27. Wahl LM, Wahl SM, Smythies LE, Smith PD. “Isolation of Human Monocyte Populations,” in *Current Protocols in Immunology*, eds. Coligan J. E., Bierer B. E., Margulies D. H., Shevach E. M., Strober W. (Hoboken, NJ, USA: John Wiley & Sons, Inc.). <https://doi.org/10.1002/0471142735.im0706as70> PMID: 18432977
28. Pabst MJ, Pabst KM, Handsman DB, Beranova-Giorgianni S, Giorgianni F. Proteome of monocyte priming by lipopolysaccharide, including changes in interleukin-1beta and leukocyte elastase inhibitor. *Proteome Sci* (2008) 6:13. <https://doi.org/10.1186/1477-5956-6-13> PMID: 18492268
29. Zhou L, Somasundaram R, Nederhof RF, Dijkstra G, Faber KN, Peppelenbosch MP, et al. Impact of human granulocyte and monocyte isolation procedures on functional studies. *Clin Vaccine Immunol CVI* (2012) 19:1065–1074. <https://doi.org/10.1128/CVI.05715-11> PMID: 22552601
30. Sarvaiya HA, Lazar IM. Insulin stimulated MCF7 breast cancer cells: Proteome dataset. *Data Brief* (2016) 9:579–584. <https://doi.org/10.1016/j.dib.2016.09.025> PMID: 27761513
31. Aribi M, Meziane W, Habi S, Boulatika Y, Marchandin H, Aymeric J-L. Macrophage Bactericidal Activities against *Staphylococcus aureus* Are Enhanced In Vivo by Selenium Supplementation in a Dose-Dependent Manner. *PLOS ONE* (2015) 10:e0135515. <https://doi.org/10.1371/journal.pone.0135515> PMID: 26340099
32. Herrera MT, Gonzalez Y, Hernández-Sánchez F, Fabián-San Miguel G, Torres M. Low serum vitamin D levels in type 2 diabetes patients are associated with decreased mycobacterial activity. *BMC Infect Dis* (2017) 17: <https://doi.org/10.1186/s12879-017-2705-1> PMID: 28882103
33. Nouari W, Ysmail-Dahlouk L, Aribi M. Vitamin D3 enhances bactericidal activity of macrophage against *Pseudomonas aeruginosa*. *Int Immunopharmacol* (2016) 30:94–101. <https://doi.org/10.1016/j.intimp.2015.11.033> PMID: 26655879
34. Aribi M. Macrophage Bactericidal Assays. *Methods Mol Biol Clifton NJ* (2018) 1784:135–149. https://doi.org/10.1007/978-1-4939-7837-3_14 PMID: 29761396
35. Kavooosi G, Ardestani SK, Kariminia A, Tavakoli Z. Production of nitric oxide by murine macrophages induced by lipophosphoglycan of *Leishmania major*. *Korean J Parasitol* (2006) 44:35. <https://doi.org/10.3347/kjp.2006.44.1.35> PMID: 16514280
36. Blond D, Raoul H, Le Grand R, Dormont D. Nitric Oxide Synthesis Enhances Human Immunodeficiency Virus Replication in Primary Human Macrophages. *J Virol* (2000) 74:8904–8912. <https://doi.org/10.1128/jvi.74.19.8904-8912.2000> PMID: 10982333

37. Takano S, Kaji H, Hayashi F, Higashiguchi K, Joukei S, Kido Y, et al. A calculation model for serum ionized calcium based on an equilibrium equation for complexation. *Anal Chem Insights* (2012) 7:23–30. <https://doi.org/10.4137/ACI.S9681> PMID: 22837641
38. Walton PA. Effects of peroxisomal catalase inhibition on mitochondrial function. *Front Physiol* (2012) 3: <https://doi.org/10.3389/fphys.2012.00108> PMID: 22536190
39. Zhuang Y, Miskimins WK. Metformin Induces Both Caspase-Dependent and Poly(ADP-ribose) Polymerase-Dependent Cell Death in Breast Cancer Cells. *Mol Cancer Res* (2011) 9:603–615. <https://doi.org/10.1158/1541-7786.MCR-10-0343> PMID: 21422199
40. Eroglu Z, Tagawa T, Somlo G. Human epidermal growth factor receptor family-targeted therapies in the treatment of HER2-overexpressing breast cancer. *The Oncologist* (2014) 19:135–150. <https://doi.org/10.1634/theoncologist.2013-0283> PMID: 24436312
41. Garofalo C, Capristo M, Manara MC, Mancarella C, Landuzzi L, Belfiore A, et al. Metformin as an adjuvant drug against pediatric sarcomas: hypoxia limits therapeutic effects of the drug. *PLoS One* (2013) 8: e83832. <https://doi.org/10.1371/journal.pone.0083832> PMID: 24391834
42. Xin W, Fang L, Fang Q, Zheng X, Huang P. Effects of metformin on survival outcomes of pancreatic cancer patients with diabetes: A meta-analysis. *Mol Clin Oncol* (2018) 8:483–488. <https://doi.org/10.3892/mco.2017.1541> PMID: 29468063
43. Gao Z-Y, Liu Z, Bi M-H, Zhang J-J, Han Z-Q, Han X, et al. Metformin induces apoptosis via a mitochondria-mediated pathway in human breast cancer cells in vitro. *Exp Ther Med* (2016) 11:1700–1706. <https://doi.org/10.3892/etm.2016.3143> PMID: 27168791
44. Marinello PC, da Silva TNX, Panis C, Neves AF, Machado KL, Borges FH, et al. Mechanism of metformin action in MCF-7 and MDA-MB-231 human breast cancer cells involves oxidative stress generation, DNA damage, and transforming growth factor β 1 induction. *Tumor Biol* (2016) 37:5337–5346. <https://doi.org/10.1007/s13277-015-4395-x> PMID: 26561471
45. Mendoza MC, Er EE, Blenis J. The Ras-ERK and PI3K-mTOR pathways: cross-talk and compensation. *Trends Biochem Sci* (2011) 36:320–328. <https://doi.org/10.1016/j.tibs.2011.03.006> PMID: 21531565
46. Miller TW, Hennessy BT, González-Angulo AM, Fox EM, Mills GB, Chen H, et al. Hyperactivation of phosphatidylinositol-3 kinase promotes escape from hormone dependence in estrogen receptor-positive human breast cancer. *J Clin Invest* (2010) 120:2406–2413. <https://doi.org/10.1172/JCI41680> PMID: 20530877
47. Mutlu M, Saatci Ö, Ansari SA, Yurdusev E, Shehwana H, Konu Ö, et al. miR-564 acts as a dual inhibitor of PI3K and MAPK signaling networks and inhibits proliferation and invasion in breast cancer. *Sci Rep* (2016) 6: <https://doi.org/10.1038/srep32541> PMID: 27600857
48. Sadeghi N, Gerber DE. Targeting the PI3K pathway for cancer therapy. *Future Med Chem* (2012) 4:1153–1169. <https://doi.org/10.4155/fmc.12.56> PMID: 22709255
49. Alimova IN, Liu B, Fan Z, Edgerton SM, Dillon T, Lind SE, et al. Metformin inhibits breast cancer cell growth, colony formation and induces cell cycle arrest in vitro. *Cell Cycle* (2009) 8:909–915. <https://doi.org/10.4161/cc.8.6.7933> PMID: 19221498
50. Al-Zaidan L, El Ruz RA, Malki AM. Screening Novel Molecular Targets of Metformin in Breast Cancer by Proteomic Approach. *Front Public Health* (2017) 5:277. <https://doi.org/10.3389/fpubh.2017.00277> PMID: 29085821
51. Baskić D, Aćimović LD, Arsenijević N. [The phagocytic activity of monocytes in different stages of breast cancer]. *Med Pregl* (2003) 56 Suppl 1:103–107.
52. Cassetta L, Pollard JW. Cancer immunosurveillance: role of patrolling monocytes. *Cell Res* (2016) 26:3–4. <https://doi.org/10.1038/cr.2015.144> PMID: 26634605
53. Al Dubayee MS, Alayed H, Almansour R, Alqaoud N, Alnamlah R, Obeid D, et al. Differential Expression of Human Peripheral Mononuclear Cells Phenotype Markers in Type 2 Diabetic Patients and Type 2 Diabetic Patients on Metformin. *Front Endocrinol* (2018) 9:537. <https://doi.org/10.3389/fendo.2018.00537> PMID: 30356719
54. Szewczyk M, Richter C, Briese V, Richter D-U. A retrospective in vitro study of the impact of anti-diabetics and cardioselective pharmaceuticals on breast cancer. *Anticancer Res* (2012) 32:2133–2138. PMID: 22593501
55. Rath M, Müller I, Kropf P, Closs EI, Munder M. Metabolism via Arginase or Nitric Oxide Synthase: Two Competing Arginine Pathways in Macrophages. *Front Immunol* (2014) 5: <https://doi.org/10.3389/fimmu.2014.00532> PMID: 25386178
56. Avtandilyan N, Javrushyan H, Petrosyan G, Trchounian A. The Involvement of Arginase and Nitric Oxide Synthase in Breast Cancer Development: Arginase and NO Synthase as Therapeutic Targets in Cancer. *BioMed Res Int* (2018) 2018:1–9. <https://doi.org/10.1155/2018/8696923> PMID: 29854802

57. Keshet R, Erez A. Arginine and the metabolic regulation of nitric oxide synthesis in cancer. *Dis Model Mech* (2018) 11:dmm033332. <https://doi.org/10.1242/dmm.033332> PMID: 30082427
58. Bułdak Ł, Łabuzek K, Bułdak RJ, Kozłowski M, Machnik G, Liber S, et al. Metformin affects macrophages' phenotype and improves the activity of glutathione peroxidase, superoxide dismutase, catalase and decreases malondialdehyde concentration in a partially AMPK-independent manner in LPS-stimulated human monocytes/macrophages. *Pharmacol Rep* (2014) 66:418–429. <https://doi.org/10.1016/j.pharep.2013.11.008> PMID: 24905518
59. Kato Y, Koide N, Komatsu T, Tumurkhuu G, Dagvadorj J, Kato K, et al. Metformin Attenuates Production of Nitric Oxide in Response to Lipopolysaccharide by Inhibiting MyD88-Independent Pathway. *Horm Metab Res* (2010) 42:632–636. <https://doi.org/10.1055/s-0030-1255033> PMID: 20560107
60. Zahzeh MR, Loukidi B, Meziane W, Haddouche M, Mesli N, Zouaoui Z, et al. Relationship between NADPH and Th1/Th2 ratio in patients with non-Hodgkin lymphoma who have been exposed to pesticides. *J Blood Med* (2015) 6:99–107. <https://doi.org/10.2147/JBM.S78759> PMID: 25878515
61. Cairns RA, Harris IS, Mak TW. Regulation of cancer cell metabolism. *Nat Rev Cancer* (2011) 11:85–95. <https://doi.org/10.1038/nrc2981> PMID: 21258394
62. Monteith GR, Davis FM, Roberts-Thomson SJ. Calcium Channels and Pumps in Cancer: Changes and Consequences. *J Biol Chem* (2012) 287:31666–31673. <https://doi.org/10.1074/jbc.R112.343061> PMID: 22822055
63. Muhammad SNH, Mokhtar NF, Yaacob NS. 15d-PGJ2 Induces Apoptosis of MCF-7 and MDA-MB-231 Cells via Increased Intracellular Calcium and Activation of Caspases, Independent of ER α and ER β . *Asian Pac J Cancer Prev APJCP* (2016) 17:3223–3228. PMID: 27509924
64. Brown D, Donaldson K, Stone V. Effects of PM10 in human peripheral blood monocytes and J774 macrophages. *Respir Res* (2004) 5: <https://doi.org/10.1186/1465-9921-5-29> PMID: 15613243
65. Gronski MA, Kinchen JM, Juncadella IJ, Franc NC, Ravichandran KS. An essential role for calcium flux in phagocytes for apoptotic cell engulfment and the anti-inflammatory response. *Cell Death Differ* (2009) 16:1323–1331. <https://doi.org/10.1038/cdd.2009.55> PMID: 19461656
66. Cross BM, Breitwieser GE, Reinhardt TA, Rao R. Cellular calcium dynamics in lactation and breast cancer: from physiology to pathology. *Am J Physiol-Cell Physiol* (2014) 306:C515–C526. <https://doi.org/10.1152/ajpcell.00330.2013> PMID: 24225884
67. França E, Honorio-França A, Nunes G, Fagundes D, Marchi P, Fernandes R, et al. Intracellular calcium is a target of modulation of apoptosis in MCF-7 cells in the presence of IgA adsorbed to polyethylene glycol. *OncoTargets Ther* (2016) 617. <https://doi.org/10.2147/OTT.S99839> PMID: 26893571
68. Dennis KL, Blatner NR, Gounari F, Khazaie K. Current status of interleukin-10 and regulatory T-cells in cancer. *Curr Opin Oncol* (2013) 25:637–645. <https://doi.org/10.1097/CCO.000000000000006> PMID: 24076584
69. Mumm JB, Emmerich J, Zhang X, Chan I, Wu L, Mauze S, et al. IL-10 elicits IFN γ -dependent tumor immune surveillance. *Cancer Cell* (2011) 20:781–796. <https://doi.org/10.1016/j.ccr.2011.11.003> PMID: 22172723
70. Mojic M, Takeda K, Hayakawa Y. The Dark Side of IFN- γ : Its Role in Promoting Cancer Immuno-evasion. *Int J Mol Sci* (2017) 19:89. <https://doi.org/10.3390/ijms19010089> PMID: 29283429
71. Olingy CE, Dinh HQ, Hedrick CC. Monocyte heterogeneity and functions in cancer. *J Leukoc Biol* (2019) 106:309–322. <https://doi.org/10.1002/JLB.4RI0818-311R> PMID: 30776148
72. Turrini R, Pabois A, Xenarios I, Coukos G, Delaloye J-F, Doucey M-A. TIE-2 expressing monocytes in human cancers. *Oncoimmunology* (2017) 6:e1303585. <https://doi.org/10.1080/2162402X.2017.1303585> PMID: 28507810
73. Ibberson M, Bron S, Guex N, Faes-van't Hull E, Ifticene-Treboux A, Henry L, et al. TIE-2 and VEGFR Kinase Activities Drive Immunosuppressive Function of TIE-2-Expressing Monocytes in Human Breast Tumors. *Clin Cancer Res* (2013) 19:3439–3449. <https://doi.org/10.1158/1078-0432.CCR-12-3181> PMID: 23649001
74. Das A, Sinha M, Datta S, Abas M, Chaffee S, Sen CK, et al. Monocyte and macrophage plasticity in tissue repair and regeneration. *Am J Pathol* (2015) 185:2596–2606. <https://doi.org/10.1016/j.ajpath.2015.06.001> PMID: 26118749
75. Mitchell AJ, Roediger B, Weninger W. Monocyte homeostasis and the plasticity of inflammatory monocytes. *Cell Immunol* (2014) 291:22–31. <https://doi.org/10.1016/j.cellimm.2014.05.010> PMID: 24962351
76. Jenkins SJ, Ruckerl D, Cook PC, Jones LH, Finkelman FD, van Rooijen N, et al. Local macrophage proliferation, rather than recruitment from the blood, is a signature of TH2 inflammation. *Science* (2011) 332:1284–1288. <https://doi.org/10.1126/science.1204351> PMID: 21566158

77. Stephen J, Emerson B, Fox KAA, Dransfield I. The uncoupling of monocyte-platelet interactions from the induction of proinflammatory signaling in monocytes. *J Immunol Baltim Md 1950* (2013) 191:5677–5683. <https://doi.org/10.4049/jimmunol.1301250> PMID: 24133165
78. Tachado SD, Li X, Swan K, Patel N, Koziel H. Constitutive activation of phosphatidylinositol 3-kinase signaling pathway down-regulates TLR4-mediated tumor necrosis factor-alpha release in alveolar macrophages from asymptomatic HIV-positive persons in vitro. *J Biol Chem* (2008) 283:33191–33198. <https://doi.org/10.1074/jbc.M805067200> PMID: 18826950
79. Kahl BC, Goulian M, van Wamel W, Herrmann M, Simon SM, Kaplan G, et al. Staphylococcus aureus RN6390 replicates and induces apoptosis in a pulmonary epithelial cell line. *Infect Immun* (2000) 68:5385–5392. <https://doi.org/10.1128/iai.68.9.5385-5392.2000> PMID: 10948168
80. Bravo-Santano N, Ellis JK, Mateos LM, Calle Y, Keun HC, Behrends V, et al. Intracellular Staphylococcus aureus Modulates Host Central Carbon Metabolism To Activate Autophagy. *mSphere* (2018) 3: <https://doi.org/10.1128/mSphere.00374-18> PMID: 30089650